


A laboratory model of the aortic root flow including the coronary arteries

Giorgio Querzoli¹  · Stefania Fortini² · Stefania Espa² · Simone Melchionna³

Received: 27 April 2016 / Revised: 25 June 2016 / Accepted: 21 July 2016 / Published online: 4 August 2016
© Springer-Verlag Berlin Heidelberg 2016

Abstract Cardiovascular flows have been extensively investigated by means of in vitro models to assess the prosthetic valve performances and to provide insight into the fluid dynamics of the heart and proximal aorta. In particular, the models for the study of the flow past the aortic valve have been continuously improved by including, among other things, the compliance of the vessel and more realistic geometries. The flow within the sinuses of Valsalva is known to play a fundamental role in the dynamics of the aortic valve since they host a recirculation region that interacts with the leaflets. The coronary arteries originate from the ostia located within two of the three sinuses, and their presence may significantly affect the fluid dynamics of the aortic root. In spite of their importance, to the extent of the authors' knowledge, coronary arteries were not included so far when modeling in vitro the transvalvular aortic flow. We present a pulse duplicator consisting of a passively pulsing ventricle, a compliant proximal aorta, and coronary arteries connected to the sinuses of Valsalva. The coronary flow is modulated by a self-regulating device mimicking the physiological mechanism, which is based on the contraction and relaxation of the heart muscle during the cardiac cycle. Results show that the model reproduces satisfyingly the coronary flow. The analysis of the time evolution of the velocity and vorticity fields within the aortic root reveals

the main characteristics of the backflow generated through the aorta in order to feed the coronaries during the diastole. Experiments without coronary flow have been run for comparison. Interestingly, the lifetime of the vortex forming in the sinus of Valsalva during the systole is reduced by the presence of the coronaries. As a matter of fact, at the end of the systole, that vortex is washed out because of the suction generated by the coronary flow. Correspondingly, the valve closure is delayed and faster compared to the case with no coronary flow.

1 Introduction

The blood flow within the aortic root and the proximal aortic artery has been extensively investigated by means of in vitro models during the last decades. Since the early sixties such models have been proposed for the assessment of the hemodynamic performances of the prosthetic valves, initially by visualization and pressure measurements (Calvert et al. 1964; Davey et al. 1966; Björk and Olin 1970), then the flow was investigated using both laser Doppler velocimetry (Yoganathan et al. 1979; Tiederman et al. 1988; Martinez-Val et al. 1990) and flow visualization. Other studies aimed at exploring the implications of the onset of turbulence on the hemolysis (Grigioni et al. 2002). More recently, the development and widespread use of the image velocimetry led to the study of the global structure of the velocity field and its time evolution (Brücker 1997; Rosenfeld et al. 2001; Balducci et al. 2004; Bellofiore et al. 2011). At the same time, the development of the diagnostic imaging techniques such as cardiovascular magnetic resonance (Kvitting et al. 2004) and three-dimensional color Doppler echocardiography (Abbas et al. 2015) gave the chance of using in vitro modeling as a support to the

✉ Giorgio Querzoli
querzoli@unica.it

¹ DICAAR, Università degli studi di Cagliari, Via Marengo 2, 09123 Cagliari, Italy

² DICEA, La Sapienza Università di Roma, Via Eudossiana 18, 00184 Rome, Italy

³ Istituto Sistemi Complessi, CNR, Via dei Taurini 19, 00185 Rome, Italy

interpretation of the clinical observations (Querzoli et al. 2014).

Laboratory models used to reproduce the flow through the aortic valve and in the aortic root underwent a corresponding development. First models consisted in closed hydraulic circuits generating a steady and/or pulsatile flow (Bellhouse and Talbot 1969; Martin et al. 1978; Reul and Black 1984). Affeld et al. (1986) designed an apparatus where the pulsatile flow was generated by the motion of a piston directly connected to the aortic orifice. More complete pulse duplicators consisted of a mock loop driven by a flexible ventricle changing volume during the cardiac cycle (Reul et al. 1981; Reul 1983). In most of former models, the aortic vessel was rigid, typically made of Perspex (Bellhouse and Talbot 1969) or blown glass (Grigioni et al. 2001; Balducci et al. 2004). More recently, the vessel was made of silicon rubber in order to reproduce the physiological compliance of the aorta (Linde et al. 2012; Gülan et al. 2012), and Querzoli et al. (2014) reproduced quantitatively the aortic distensibility observed in vivo during the cardiac cycle.

The sinuses of Valsalva have been recognized to play a key role in the fluid dynamics of the aortic root since the pioneering work of Bellhouse and Talbot (1969), who suggested an influence in the closure of the valve, until the recent study by Moore and Dasi (2014) which was focused on the features of the vortexes developing within the sinuses. Furthermore, Querzoli et al. (2014) suggested a redirection of the systolic transvalvular jet due to those structures.

However, another fundamental function of the sinuses of Valsalva is hosting the origin of the coronary arteries. As a matter of fact, the two major vessels of the coronary circulation, the left and right main coronary arteries, originate from openings called the coronary ostia, located inside the left and right Valsalva sinus, respectively. No vessels originate from the third sinus, which is therefore referred to as non-coronary sinus. Coronary arteries lie on the surface of the heart and bifurcate in a compact network of branches constituting the coronary circulation, which distribute the oxygenated blood to every part of the cardiac muscle. The structure of the network is widely variable among individuals, and a complex physiologic mechanism regulates the coronary flow depending on the working conditions of the heart. Therefore, obtaining a reliable relationship between pressure and flow rate under different conditions is not a trivial task and most of studies in the literature are based on in vivo investigations (Zamir 2006).

Kleine et al. (2002) investigated the influence of bi-leaflet and tilting disk valve orientation on coronary artery flow in pigs. They found that coronary blood flow was dependent on the valve orientation and showed the optimum setup for each prosthetic valve model. De Paulis et al. (2004)

carried out an in vivo study of coronary flow after aortic root replacement suggesting a role of the sinuses in the modulation of the coronary flow during the cycle. De Tullio et al. (2011) investigated by means of numerical simulations the effect of aortic root geometry on the coronary entry flow after a bi-leaflet mechanical heart valve graft; they found that the geometry of the aortic root affects meaningfully the pressures in the proximity of the coronary ostia. Nevertheless to the authors' knowledge, no in vitro models including the coronary arteries have been described in the literature so far; the aim of this paper is to try to fill that gap.

Hereafter, we present a pulse duplicator, consisting of a passively pulsing ventricle, a compliant proximal aorta, and coronary arteries connected to the sinuses of Valsalva. The coronary flow is modulated by mimicking the physiological mechanism, which is based on the contraction and relaxation of the heart muscle during the cardiac cycle.

The coronary circulation depends on two main factors: blood pressure within the aortic root and vascular resistance. The former is primarily determined by the variation of the intraventricular pressure, with a maximum value attained during the systole and lower values during the diastole. The latter depends on the cyclic compression of coronary vessels by the heart muscle, which is a maximum during the systolic contraction. The resulting flow rate is very low during the whole systole and exhibits a sudden peak at the beginning of the diastolic relaxation. Then, the flow rate gradually decreases because of the behavior of the aortic pressure. Thus, most of the coronary blood flow occurs during the diastole (Rubio and Berne 1975).

The pulse duplicator described here is a development of that used in previous investigations of intraventricular (Cenedese et al. 2005; Querzoli et al. 2010; Vukićević et al. 2012; Fortini et al. 2013) and aortic flow (Querzoli et al. 2014). The study was performed by using an aortic root model equipped with a bi-leaflet mechanical prosthetic valve. In a first series of experiments, coronary arteries were left open. Then, the coronaries were clamped to comparatively evaluate the effect of the coronary flow in the fluid dynamics of the aortic root.

2 Materials and methods

The pulse duplicator reproduces the flow both within the left ventricle and through the proximal aorta (Fig. 1). The fluid flow is generated by the periodic volume change of the ventricle (V), which is housed in a closed chamber (A) with 20-mm-thick Plexiglas walls, filled with water, and communicating with a piston driven by a linear motor (LM). The linear motor is controlled in velocity by a personal computer and moves according to a speed law

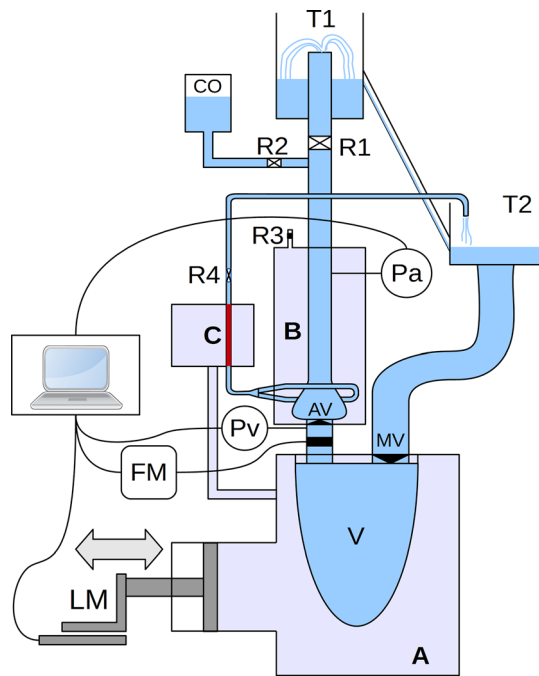


Fig. 1 Sketch of the pulse duplicator. *A* Ventricular tank; *B* aortic tank; *C* coronary tank; *AV* aortic valve; *T1* and *T2* aortic and atrial tank; *MV* mitral valve; *V* ventricle; *CO* compliance; *R1–R4* adjustable resistances; *LM* linear motor; *Pa* and *Pb* pressure probes; *FM* electromagnetic flowmeter

digitally assigned. The ventricle is a flexible sack made of silicon rubber. Since the ventricular chamber (*A*) is filled with an incompressible fluid, the changes of volume of the ventricle are directly correspondent to the stroke volume of the piston. Two valves are placed at the inlet and outlet of the ventricle (for further details, refer to Fortini et al. 2013 and references therein). During the present experiments, a hydraulic check valve was placed in mitral position (*MV*) while a prosthetic bi-leaflet mechanical valve was used as aortic valve (*AV*) (Sorin Bicarbon, 27 mm nominal diameter). From the ventricle, the working fluid flows through the model proximal aorta that is made of silicone rubber and is housed in a chamber (*B*) with 10-mm-thick Plexiglas walls filled with water. The distensibility of the aortic model was controlled by means of a vertical tube that connected the aortic chamber with the atmosphere. As the water flowed through the resistance, the model aorta dilated. The resistance (*R3*), along the vertical tube, was tuned to reproduce the distensibility of a healthy aorta during the cardiac cycle (Querzoli et al. 2014). Downstream of the model aorta, a resistance (*R1*) and a compliance (*CO*) connected to the aortic conduit through a second resistance (*R2*) reproduce the impedance of the systemic circulation. The aortic conduit terminates with a constant head reservoir (*T1*) that feeds a second reservoir (*T2*) connected to the mitral valve (*MV*).

The model aorta includes two coronary arteries originating from the sinuses of Valsalva, which are connected to the tank (*T2*). The regulation of the coronary flow is obtained by means of the chamber (*C*), directly connected to the ventricular chamber (*A*). The water inside the chamber simulates the compression of the coronary vessel by the cardiac muscle: During the systole the ventricular pressure increases, closing the tract of the tube inside the chamber (*C*). Correspondingly, the coronary flow is stopped. Conversely, during the diastole, the ventricular pressure is low, the vessel is completely open, and the coronary flow rate is a maximum. A resistance (*R4*) allows for the tuning of the regulating device. Two piezoelectric sensors (*Pv* and *Pa*), located just upstream and 6.5 aortic diameters downstream of the valve, probed the ventricular and aortic pressure, respectively. An electromagnetic flowmeter (*FM*) recorded the flow rates during the cardiac cycle.

Distilled water was used as working fluid (9.0 g of sodium chloride per liter were added in order to meet the flowmeter operating requirements). The geometric scale was 1:1. The non-dimensional parameters controlling the dynamic similarity are the Reynolds ($Re = UD/\nu$) and Womersley ($Wo = D/\sqrt{T\nu}$) numbers; where $D = 27$ mm is the aortic diameter, U the peak velocity through the aortic orifice, T the period of the cardiac cycle, and ν the kinematic viscosity of the working fluid.

Furthermore, a second Reynolds number, Re_a , based on the velocity averaged during the whole cycle, can be defined. Since the kinematic viscosity of water is about three times lower than that of blood, the dynamic similarity was obtained by fixing the stroke volume (*SV*) in the physiological range and lowering to one-third the target beat rate. Experiments were run in order to simulate a beat rate of 75 beats per min and a cardiac output of 4.8 L per min. The compliance *CO* and the resistances *R1* and *R2* were adjusted to obtain a 100 mmHg mean aortic pressure (measured by the probe *Pb*). Main working parameters are listed in Table 1.

In order to measure the velocity field, a vertical plane including the axis of both the proximal left coronary artery and the aortic root was illuminated by a 12 W infrared laser (800 nm wavelength). The working fluid was seeded

Table 1 Experimental parameters

<i>SV</i>	64 mL
<i>T</i>	2.4 s
ν	10^{-6} m ² /s
<i>U</i>	0.11 m/s
<i>Wo</i>	17
<i>Re</i>	2900
Re_a	1590

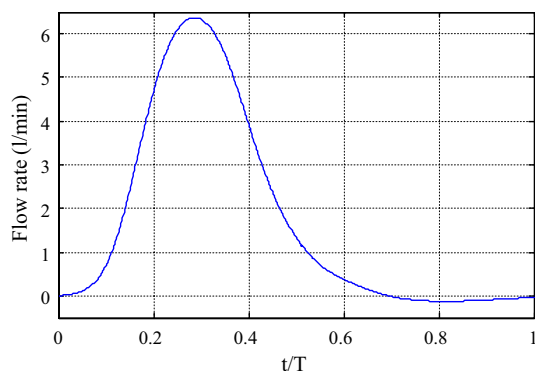


Fig. 2 Aortic flow rate as a function of non-dimensional time. Maximum uncertainty in the phase average evaluation reached during the cycle is $\pm 6.9 \times 10^{-3}$ L/min

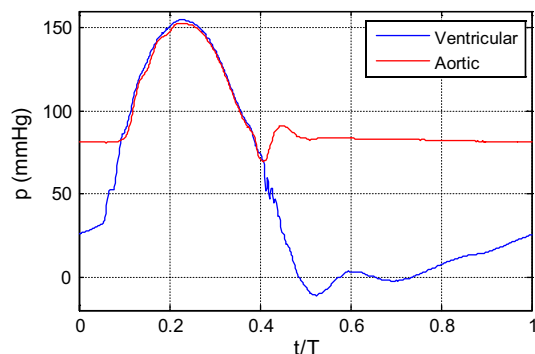


Fig. 3 Ventricular and aortic pressures measured by (Pa) and (Pb) transducers, respectively. Maximum uncertainty in the phase average evaluation reached during the cycle is ± 1.5 and ± 0.4 mmHg for the ventricular and aortic pressure, respectively

with neutrally buoyant particles ($50 \mu\text{m}$ average diameter). Series of images were acquired by a high-speed camera at 450 Hz frame-rate and a spatial resolution of 1280×1024 pixels. A feature tracking algorithm (Cenedese et al. 2005) was used to measure the instantaneous velocity field by recognizing particles trajectories. Interpolation of sparse data on a regular 50×51 grid provided the 2D Eulerian velocity field at each time instant. One hundred consecutive cycles have been acquired, and phase averages will be presented hereafter.

The law of motion of the piston controlling the ventricular volume was the same as in previous studies (Querzoli et al. 2014), designed to mimic a physiological systolic flow through the aorta, and with a reduced duration of the diastole compared to typical values. The measured flow rate is plotted in Fig. 2 as a function of non-dimensional time. The systolic peak is attained at $t = 0.29 T$, and a moderate leakage backflow is observed during the diastole. The corresponding aortic and ventricular pressures are

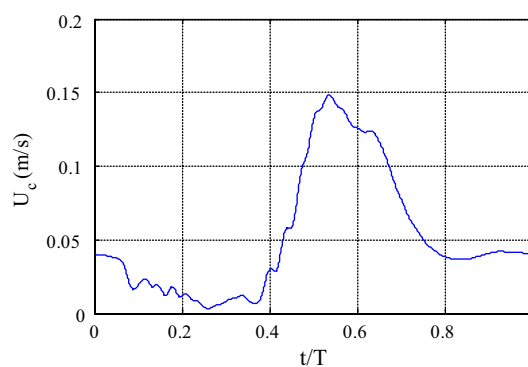


Fig. 4 Average velocity at the inlet of the coronary artery as a function of the non-dimensional time. Maximum uncertainty in the average evaluation reached during the cycle is $\pm 1.5 \times 10^{-3}$ m/s

plotted in Fig. 3. The ventricular pressure exceeds the aortic one at $t = 0.09 T$, when the valve opens. At $t = 0.41 T$, the aortic pressure returns greater than the ventricular one, the valve closes, and the typical notch is observed in the aortic pressure. The time evolution of the average velocity immediately downstream the left coronary ostium, U_c , plotted in Fig. 4, confirms that the mechanism modulating the coronary flow successfully mimics the effect of the contraction of the heart muscle on the coronary circulation. Most of the flow occurs during the diastole (Matsuo et al. 1988; Kajiya et al. 1993), whereas during the systole, U_c is low and continuously decreasing since the high pressure in the chamber (C) squeezes the coronary conduit increasing the resistance of the coronary circulation. A sudden increase is observed at $t = 0.38 T$, just before the closure of the aortic valve, and it is a maximum during the diastole ($t = 0.53 T$).

3 Results

The streamlines and velocity magnitude made non-dimensional by the peak velocity through the aortic orifice, U , are plotted in Fig. 5 at six points of the cardiac cycle.

During the initial stage of the systole (Fig. 5a), the bileaflet valve opens and three jets propagate through the aortic root, and a well-defined recirculating vortex is formed in the sinus of Valsalva with a small secondary recirculation pattern at the coronary ostium. No flow is observed in the coronary artery.

At the systolic peak (Fig. 5b), the valve is completely open and the systolic flow well developed. The central and left jets merge together, whereas the right jet remains isolated and impinges the wall at the height of the sinotubular junction, then propagating along the wall of the proximal aorta. Also, at this time no meaningful flow is observed through the coronary artery. Just after the valve closure

Fig. 5 Color plot of the non-dimensional velocity magnitude, u/U , at six time instants of the cardiac cycle. The streamlines are superimposed. **a** $t/T = 0.16$, **b** $t/T = 0.29$, **c** $t/T = 0.43$, **d** $t/T = 0.54$, **e** $t/T = 0.63$, **f** $t/T = 0.98$. The insert in the *bottom left* of the panels indicates with a *red dot* the corresponding point of flow rate cycle

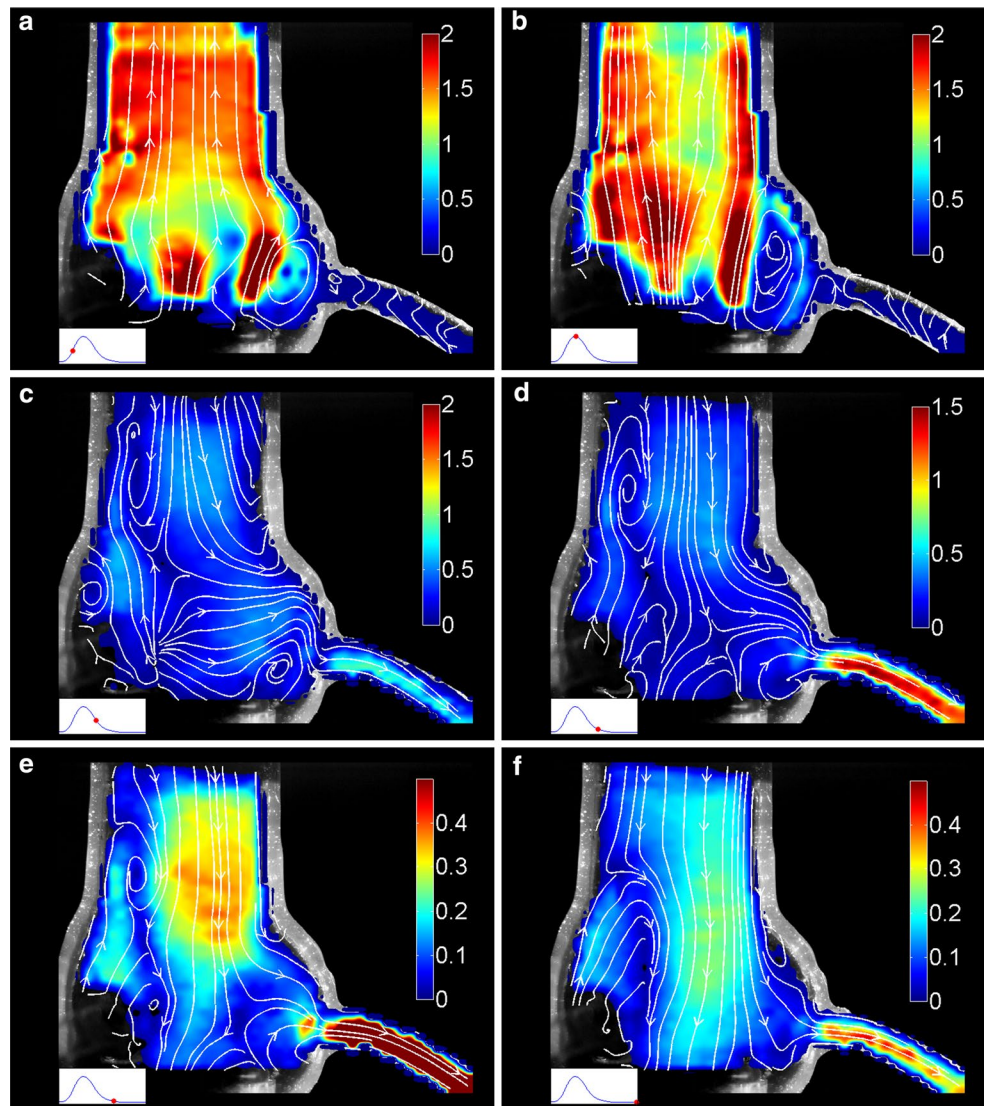


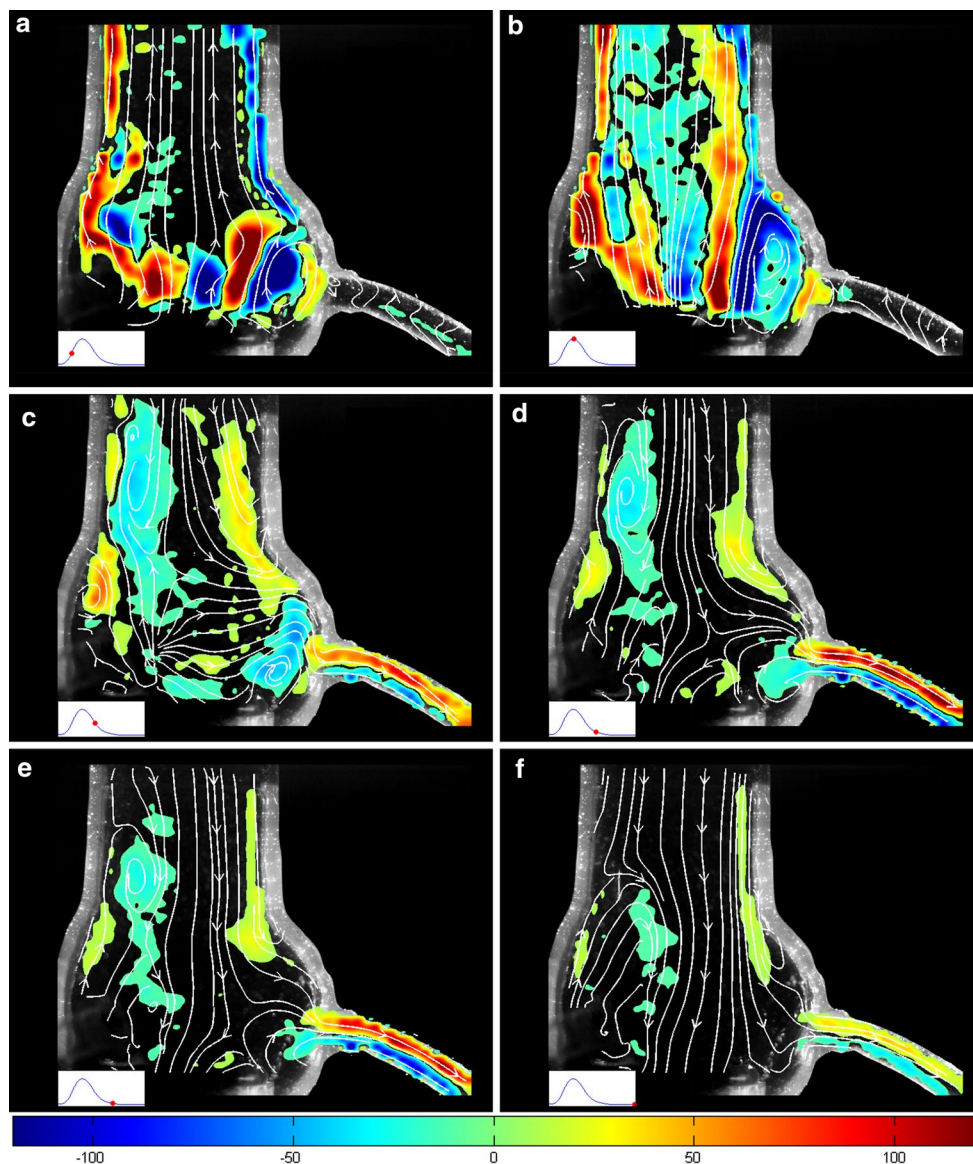
(Fig. 5c), the coronary flow starts and it is initially fed by the residual flow from the valve.

As the transvalvular flow terminates completely (Fig. 5d) and the coronary flow increases, the coronary circulation is mainly fed by the backflow from the aorta. At the beginning of the diastole (Fig. 5e), the backflow entering the coronary artery develops mainly on the sinus side of the aortic vessel (right of the plot) and generates a small recirculation region at the sinotubular junction, close to the sinus of Valsalva. On the opposite side (left of the plot), a wide region of weak recirculation is observed. Streamlines indicate that the coronary flow is fed partially from the valve leakage. At the end of diastole (Fig. 5f), the coronary flow is decreasing and originates entirely from the aorta. Also, at that stage, the backflow is more intense on the right side of the vessel, whereas on the opposite side, close to the commissure, the large region of weak recirculation persists.

Out-of-plane vorticity maps plotted in Fig. 6 exhibit high vorticity layers adjacent to the aortic walls during the accelerated systole (Fig. 6a) and during the backflow (Fig. 6c, d). During the whole systole, clockwise vorticity resides in the sinus of Valsalva, until it is washed out by the coronary flow. A peak of counter-clockwise vorticity is observed on the right of the sinotubular junction, due to the small recirculation region at the downstream end of the sinus (Fig. 6e, f).

In order to highlight the effect of the coronary flow, a second series of measurements was taken with the coronary vessels clamped in order to have no coronary flow. The two most significant time instants are shown in Fig. 7 together with the corresponding instants of the case with coronary flow. The overall structure of the flow field in Fig. 7a, c is similar to that observed in Fig. 7b, d, respectively. The main difference consists in the presence of the clockwise

Fig. 6 Streamlines and distribution of out-of-plane vorticity made non-dimensional by the inverse of the period, T , at the same time instants as in Fig. 5



recirculation region within the sinus of Valsalva, which, in this case, is not washed out through the coronary artery.

The cumulative effect of the presence of the coronary on the flow in aortic root is shown in Fig. 8 where the vorticity fields, averaged over systolic ejection and diastolic phases, are comparatively presented in the case of presence or not of coronary flow. During the systole, the two series of experiments gave similar results (Fig. 8a, b) except in the coronary artery, where the vorticity generated by the boundary layer within the vessel is clearly apparent. During the diastole, the coronary flow experiments exhibit high vorticity levels within the coronary vessel. Compared to the experiments without coronary flow, a higher vorticity region is observed at the sinotubular junction, on the right side of the plot, because of the recirculation generated by the backflow from the proximal aorta, which feeds the

coronary vessel. Both during systole and diastole, the average clockwise vorticity within the sinus of Valsalva is highest for the experiments with coronary flow.

4 Discussion

We proposed a mock loop reproducing in vitro the blood flow in the aortic root, which includes the presence of the coronary arteries. The coronary flow is modulated by a self-regulation device mimicking the physiological compression of the coronary circulation by the heart muscle. As shown in Fig. 1, the modulation is driven by the difference between the ventricular and the coronary pressure. Though the coronary flow is highly variable among individuals, the mock loop presented here is able to satisfyingly reproduce

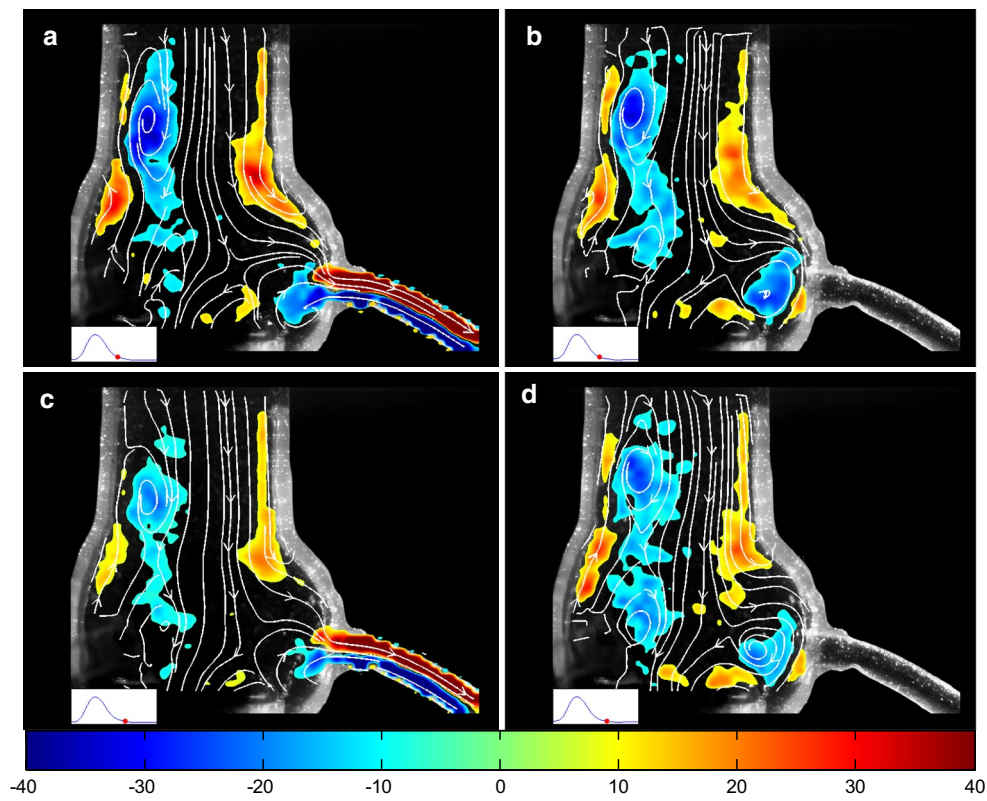
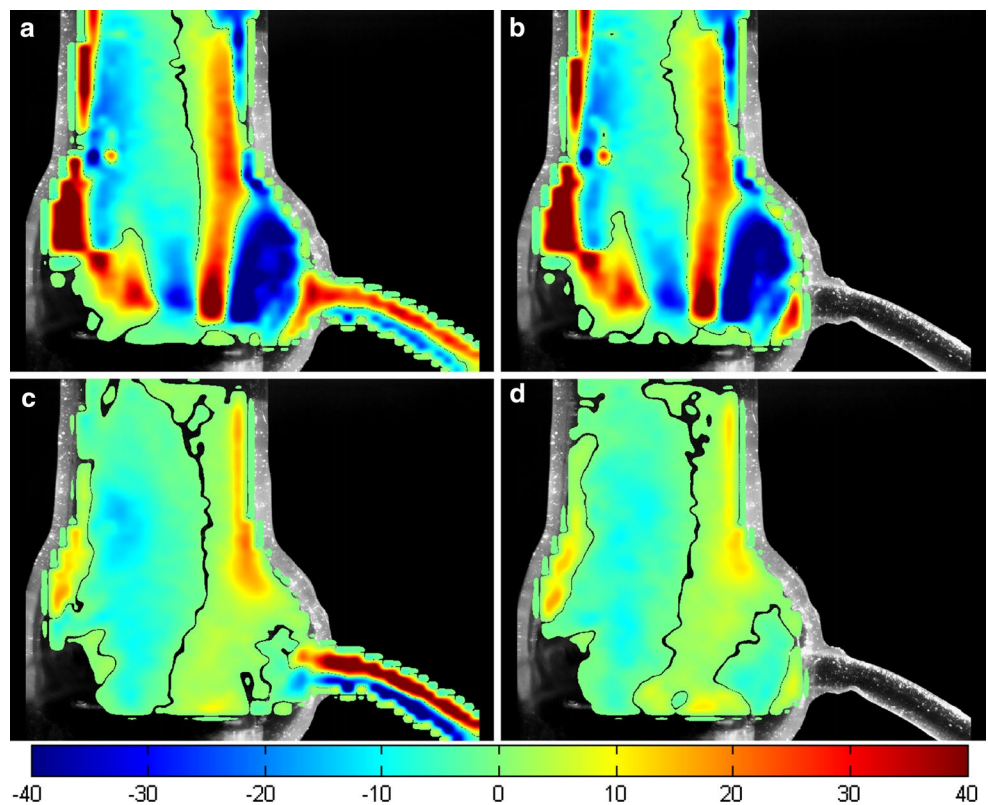


Fig. 7 Streamlines and dimensionless out-of-plane vorticity distribution in experiments run with (*left panels*) and without (*right panels*) the coronary flow at $t/T = 0.54$ (**a, b**) and $t/T = 0.63$ (**c, d**). Vorticity is non-dimensionalized by the inverse of the period, T

Fig. 8 Average dimensionless out-of-plane vorticity during the systolic ejection (**a, b**) and diastole (**c, d**). *Left plots a, c* show the experiments with coronary flow, *right plots b, d* show the experiments without coronary flow



its fundamental features (Fig. 4). In particular, as in healthy coronaries, the coronary velocity is low during the whole systole, and most of flow occurs during the diastole (about 75 %).

The analysis of the time evolution of the velocity field unveils the role of the coronaries in the fluid dynamics of the aortic root. As expected, during the systole, no prominent effects are observed but for a secondary (counter-clockwise) vortical region hosted by the inlet of the coronary vessel, i.e., the ostium (Fig. 6b). That vortex is driven by the main, clockwise, recirculation dominating the sinus of Valsalva.

At its initial stage, the coronary flow is fed partly by the residual flow through the aortic valve and for the remaining portion by a backflow from the aorta. These two flows are separated by a saddle point that moves toward the aortic annulus as the valve closes and the transvalvular flow becomes vanishingly small (Fig. 5c–e). The backflow develops along the aortic vessel mainly on the same side of the sinus (right of the plot). On the opposite side of the aorta, i.e., close to the wall above the commissure (left of the plot), a large recirculating zone, characterized by a couple of vortices, contributes to redirect the flow toward the sinus (Fig. 6c, d).

Comparison of the velocity fields obtained in series of experiments run with (Figs. 5, 6e, f), and without (Fig. 7a, b), the coronary flow unveils that the recirculating vortex, generated during the systolic ejection in sinus of Valsalva, vanishes earlier because it is washed out through the coronary vessel during the diastole. This effect is confirmed by the analysis of the diastolic average vorticity maps (Fig. 8c, d), which exhibit lower values of clockwise (negative) vorticity within the sinus of Valsalva.

It is well known that the recirculation in the sinus of Valsalva plays a role in the closure of the valve by interacting with the moving leaflets (Bellhouse and Talbot 1969; Robicsek 1991; Ohta et al. 2000). As a consequence, the early vanishing of the vortex due to the suction by the coronary flow may play a meaningful role in the valve dynamics. To test this hypothesis, image sequences have been analyzed in order to compute the opening and closing times of the leaflets. The opening starts at $t = 216$ ms and leaflets take 183 ms to complete the opening, irrespective of the presence of the coronary flow. Also, the time of complete closure of the leaflets ($t = 988$ ms) is not affected by the presence of the coronary flow. Conversely, leaflets begins the closing motion at $t = 799$ ms with the coronary flow, and at $t = 777$ when the coronary flow is inhibited. The anticipated and slower (by 22 ms) closure of the leaflets observed in the absence of coronary flow can be ascribed to the role of the vortex persisting in the sinus of Valsalva. These results suggest that the coronary flow should be

accurately reproduced when simulating the blood flow in the aortic root.

Acknowledgments This work was partially funded by the Ministero dell'Istruzione, dell'Università e della Ricerca (IT). PRIN 2012, Grant No. 2012HMR7CF.

References

- Abbas AE, Franey LM, Lester S et al (2015) The role of jet eccentricity in generating disproportionately elevated transaortic pressure gradients in patients with aortic stenosis. *Echocardiography* 32:372–382. doi:10.1111/echo.12712
- Affeld K, Spiegelberg A, Schichl K, Mohnhaupt A (1986) Design of a new tester for artificial heart valves. *Life Support Syst* 4:142–144
- Balducci A, Grigioni M, Querzoli G et al (2004) Investigation of the flow field downstream of an artificial heart valve by means of PIV and PTV. *Exp Fluids* 36:204–213. doi:10.1007/s00348-003-0744-4
- Bellhouse BJ, Talbot L (1969) The fluid mechanics of the aortic valve. *J Fluid Mech* 35:721–735. doi:10.1017/S0022112069001406
- Bellofiore A, Donohue EM, Quinlan NJ (2011) Scale-up of an unsteady flow field for enhanced spatial and temporal resolution of PIV measurements: application to leaflet wake flow in a mechanical heart valve. *Exp Fluids* 51:161–176. doi:10.1007/s00348-010-1038-2
- Björk VO, Olin C (1970) Hydrodynamic comparison between the new tilting disc aortic valve prosthesis (Björk–Shiley) and the corresponding prostheses of Starr–Edwards, Kay–Shiley, Smeloff–Cutter and Wada–Cutter in the pulse duplicator. *Scand J Thorac Cardiovasc Surg* 4:31–36. doi:10.3109/14017437009134237
- Brücker C (1997) Dual-camera DPIV for flow studies past artificial heart valves. *Exp Fluids* 22:496–506. doi:10.1007/s003480050077
- Calvert G, Drabble J, Serafin R, Temple LJ (1964) An aortic pulse duplicator of simple design. *J Thorac Cardiovasc Surg* 47:633–643
- Cenedese A, Prete ZD, Miozzi M, Querzoli G (2005) A laboratory investigation of the flow in the left ventricle of a human heart with prosthetic, tilting-disk valves. *Exp Fluids* 39:322–335. doi:10.1007/s00348-005-1006-4
- Davey TB, Kaufman B, Smeloff EA (1966) Pulsatile flow studies of prosthetic heart valves. *J Thorac Cardiovasc Surg* 51:264–267
- de Tullio MD, Pedrizzetti G, Verzicco R (2011) On the effect of aortic root geometry on the coronary entry-flow after a bileaflet mechanical heart valve implant: a numerical study. *Acta Mech* 216:147–163. doi:10.1007/s00707-010-0361-2
- Fortini S, Querzoli G, Espa S, Cenedese A (2013) Three-dimensional structure of the flow inside the left ventricle of the human heart. *Exp Fluids* 54:1–9. doi:10.1007/s00348-013-1609-0
- Grigioni M, Daniele C, D'Avenio G, Barbaro V (2001) The influence of the leaflets' curvature on the flow field in two bileaflet prosthetic heart valves. *J Biomech* 34:613–621. doi:10.1016/S0021-9290(00)00240-2
- Grigioni M, Daniele C, D'Avenio G, Barbaro V (2002) Monodimensional estimation of maximum Reynolds shear stress in the downstream flow field of bileaflet valves. *J Heart Valve Dis* 11:392–401
- Gülan U, Lüthi B, Holzner M et al (2012) Experimental study of aortic flow in the ascending aorta via Particle Tracking Velocimetry. *Exp Fluids* 53:1469–1485. doi:10.1007/s00348-012-1371-8

- Kajiya F, Matsuoka S, Ogasawara Y et al (1993) Velocity profiles and phasic flow patterns in the non-stenotic human left anterior descending coronary artery during cardiac surgery. *Cardiovasc Res* 27:845–850. doi:[10.1093/cvr/27.5.845](https://doi.org/10.1093/cvr/27.5.845)
- Kleine P, Scherer M, Abdel-Rahman U et al (2002) Effect of mechanical aortic valve orientation on coronary artery flow: comparison of tilting disc versus bileaflet prostheses in pigs. *J Thorac Cardiovasc Surg* 124:925–932. doi:[10.1067/mtc.2002.126046](https://doi.org/10.1067/mtc.2002.126046)
- Kvitting J-PE, Ebbens T, Wigström L et al (2004) Flow patterns in the aortic root and the aorta studied with time-resolved, 3-dimensional, phase-contrast magnetic resonance imaging: implications for aortic valve-sparing surgery. *J Thorac Cardiovasc Surg* 127:1602–1607. doi:[10.1016/j.jtcvs.2003.10.042](https://doi.org/10.1016/j.jtcvs.2003.10.042)
- Linde T, Hamilton KF, Navalon EC et al (2012) Aortic root compliance influences hemolysis in mechanical heart valve prostheses: an in vitro study. *Int J Artif Organs* 35:495–502. doi:[10.5301/ijao.5000108](https://doi.org/10.5301/ijao.5000108)
- Martin T, Palmer J, Black M (1978) A new apparatus for the in vitro study of aortic valve mechanics. *Eng Med* 7:229–230
- Martinez-Val R, Viedma A, Cuerno C (1990) Eulerian and Lagrangian description of a pulsatile, partially turbulent flow. *Exp Fluids* 9:129–136. doi:[10.1007/BF00187412](https://doi.org/10.1007/BF00187412)
- Matsuo S, Tsuruta M, Hayano M et al (1988) Phasic coronary artery flow velocity determined by Doppler flowmeter catheter in aortic stenosis and aortic regurgitation. *Am J Cardiol* 62:917–922. doi:[10.1016/0002-9149\(88\)90893-4](https://doi.org/10.1016/0002-9149(88)90893-4)
- Moore B, Dasi LP (2014) Spatiotemporal complexity of the aortic sinus vortex. *Exp Fluids* 55:1–12. doi:[10.1007/s00348-014-1770-0](https://doi.org/10.1007/s00348-014-1770-0)
- Ohta Y, Kikuta Y, Shimooka T et al (2000) Effect of the sinus of Valsalva on the closing motion of bileaflet prosthetic heart valves. *Artif Organs* 24:309–312. doi:[10.1046/j.1525-1594.2000.06534-2.x](https://doi.org/10.1046/j.1525-1594.2000.06534-2.x)
- Paulis RD, Tomai F, Bertoldo F et al (2004) Coronary flow characteristics after a Bentall procedure with or without sinuses of Valsalva. *Eur J Cardiothorac Surg* 26:66–72. doi:[10.1016/j.ejcts.2004.04.031](https://doi.org/10.1016/j.ejcts.2004.04.031)
- Querzoli G, Fortini S, Cenedese A (2010) Effect of the prosthetic mitral valve on vortex dynamics and turbulence of the left ventricular flow. *Phys Fluids* (1994–Present) 22:41901. doi:[10.1063/1.3371720](https://doi.org/10.1063/1.3371720)
- Querzoli G, Fortini S, Espa S et al (2014) Fluid dynamics of aortic root dilation in Marfan syndrome. *J Biomech* 47:3120–3128. doi:[10.1016/j.jbiomech.2014.06.025](https://doi.org/10.1016/j.jbiomech.2014.06.025)
- Reul H (1983) In vitro evaluation of artificial heart valves. In: Ghista DN, Yang W-J, van Vollenhoven E, Reul H, Bleifeld W (eds) *Cardiovascular engineering. Part I: modelling*. Karger, Basel
- Reul H, Black M (1984) The design, development and assessment of heart valve substitutes. In: *Proceedings of the 2nd international conference on application of physics to medicine and biology*. World Scientific Publishing, Singapore
- Reul H, Talukder N, Müller EW (1981) Fluid mechanics of the natural mitral valve. *J Biomech* 14:361–372. doi:[10.1016/0021-9290\(81\)90046-4](https://doi.org/10.1016/0021-9290(81)90046-4)
- Robicsek F (1991) Leonardo da Vinci and the sinuses of Valsalva. *Ann Thorac Surg* 52:328–335. doi:[10.1016/0003-4975\(91\)91371-2](https://doi.org/10.1016/0003-4975(91)91371-2)
- Rosenfeld M, Avrahami I, Einav S (2001) Unsteady effects on the flow across tilting disk valves. *J Biomech Eng* 124:21–29. doi:[10.1115/1.1427696](https://doi.org/10.1115/1.1427696)
- Rubio R, Berne RM (1975) Regulation of coronary blood flow. *Prog Cardiovasc Dis* 18:105–122. doi:[10.1016/0033-0620\(75\)90001-8](https://doi.org/10.1016/0033-0620(75)90001-8)
- Tiederman WG, Privette RM, Phillips WM (1988) Cycle-to-cycle variation effects on turbulent shear stress measurements in pulsatile flows. *Exp Fluids* 6:265–272. doi:[10.1007/BF00187366](https://doi.org/10.1007/BF00187366)
- Vukićević M, Fortini S, Querzoli G et al (2012) Experimental study of an asymmetric heart valve prototype. *Eur J Mech B Fluids* 35:54–60. doi:[10.1016/j.euromechflu.2012.01.014](https://doi.org/10.1016/j.euromechflu.2012.01.014)
- Yoganathan AP, Corcoran WH, Harrison EC (1979) In vitro velocity measurements in the vicinity of aortic prostheses. *J Biomech* 12:135–152. doi:[10.1016/0021-9290\(79\)90153-2](https://doi.org/10.1016/0021-9290(79)90153-2)
- Zamir M (2006) *The physics of coronary blood flow*. Springer Science & Business Media, Berlin